Kinematic, Thermodynamic and Structural Factors Governing the Dispersion of Nanoclays in Polymer Melts

Modified on Sunday, 03 May 2015 12:23 AM by mpieler — Categorized as: Paper of the Month

Kinematic, Thermodynamic and Structural Factors Governing the Dispersion of Nanoclays in Polymer Melts

Mark D. Wetzel
DuPont, Wilmington, Delaware, 19880

Abstract

Polymer nanocomposites offer a potential unique solution to improve desired physical attributes while maintaining other incompatible properties. For example, increasing the mechanical stiffness and strength of ionomers while preserving toughness and optical performance may not be possible with conventional, micron-scale fillers. In order to demonstrate significant property enhancements, a well-controlled dispersion of nano-scale fillers in a polymer matrix is required. Melt processing represents the most economical and flexible route to producing thermoplastic nanocomposites, but may not achieve dispersion quality as has been demonstrated by other methods. This paper describes melt compounding experiments that help establish kinematic, thermodynamic and structural factors that govern the dispersion of layered silicates in ionomers. The results show that the stress imparted during the melt blending influences dispersion. Platelet size also influences the extent of exfoliation in the extruder. However, the thermodynamic compatibility between the filler surface, organic modifier and matrix polymer plays a dominant role in the exfoliation process.

Introduction

In order to demonstrate significant property enhancements, a well-controlled dispersion of a nano-filler into a polymer matrix is required. A good dispersion can be characterized by a particle size distribution approaching primary particle dimensions distributed uniformly through the host polymer. For layered silicates, the process must first break apart and wet large aggregates of tactoids (cohesive platelet stacks) and then exfoliate platelets (delaminate) from the tactoids. For a given shaping and forming process (injection molding, blown film, extruded film, etc.) an anisotropic nanocomposite structure will be created with platelets and tactoids aligning with a shear or extensional flow field. Physical properties of interest depend on intrinsic matrix and filler properties, interfacial adhesion between the filler, surface modifier and polymer, the state of dispersion and particle orientations induced by processing [1-3]. Melt processing represents an economical and flexible route for producing thermoplastic nanocomposites. However, conventional melt compounding systems usually cannot create dispersions of the same quality as made with solution or in-situ polymerization methods. Thus, a conventional melt blending system may represent a tradeoff between economics and dispersion quality. To date, few, if any academic or commercial publications have achieved perfect exfoliation of layered silicates in thermoplastics using conventional batch mixers or extruders. In compounding experiments, organically modified layered silicates were dispersed into ethylene copolymer ionomers using a twin-screw extrusion process. The extent of exfoliation was examined by microscopy and through tensile property measurements of injection molded samples. This work reproduces and extends research on ionomer / clay nanocomposites conducted by Paul and associates [4-6]. They investigated the effects of counter-ion type (Li, Na, Zn) in Surlyn® ethylene copolymers along with the type of quaternary ammonium organic modifier on Montmorillonite (MMT) clay. Kamal and his co-authors reported that the thermodynamic interactions between the clay, modifier and polymer have a significant effect on the cohesive force between platelets by changing the van der Waals forces and the inter-gallery spacing [1]. Furthermore, they quantified the stress required in a polymer melt under simple shear to promote delamination of platelets or separation of child tactoids from parent particles.

Experimental

A ZSK-18mm intermeshing, co-rotating twin-screw extruder (Coperion GmbH, Stuttgart, Germany) fitted with 10 barrels was used to compound ethylene copolymer ionomers with organically modified layered silicates. A conventional compounding screw with a 41 L/D was used with a melting zone followed by one mixing section comprised of kneading blocks and reverse conveying elements. DuPont Surlyn® (partially neutralized ethylene/methacrylic acid copolymer) sodium 8945 (4.5 g/10 min at 190°C melt index) and zinc 9945 (4 g/10 min at 190°C melt index) ionomers were selected based on Paul's work [4-6]. Several 2:1 layered silicates, including organically modified Montmorillonite (MMT: Cloisite® 20A, 15A, 6A and 93A), unmodified MMT (Cloisite Na+) and synthetic Hectorite (Laponite® RD and OG) and fluorohectorite (Laponite B) were supplied by Southern Clay Products, Gonzalez, Texas. Cloisite 93A uses a more polar methyl, dihydrogenated tallow ammonium surfactant (designated MH(HT)2 with one methyl group replaced by one hydrogen) while all other clays were ion exchanged with a dimethyl, dihydrogenated tallow, quaternary ammonium moiety (designated M2(HT)2). Clay types, modifier type, amount exchanged and inter-gallery spacing measured by wide angle X-ray scattering (WAXS) are listed in Table 1.

The ingredients were added using two loss-in-weight feeders, with polymer pellets metered into the first feed port and

clay powders side-fed into barrel #4 into the molten ionomer for most tests. Several tests fed both materials in the rear feed port. The total feed rate was varied from approximately 4.5 to 9 kg/hr (10 to 20 lb/hr) with a range of powder concentrations from 3 to 10 weight percent clay content. The extruder screw speed was fixed at 350 RPM for all states, with the exception of a 9 kg/hr / 700RPM run. Barrel temperatures were fixed between 160 to 220°C from inlet to the die. In several tests, 25 wt. % Cloisite 20A masterbatches were prepared with melt mixing zone barrel temperatures set to 160 and 210°C to emulate high and low stress states, respectively. The concentrates were then let down to final compositions in a second extrusion step. Pellet samples were collected, dried and then molded into ASTM tensile bars using an Arburg Allrounder 1.5oz injection molding machine using standard Surlyn drying and operating conditions. Tensile data were measured using ASTM standard 638D on dry as molded samples. Transmission Electron Microscopy (TEM) micrographs were made with approximately 90nm thick microtomed cross-sections cut from the center of the bars, perpendicular to the flow direction.

Discussion of Results

Process Kinematic Effects

Figure 1 shows the shear stress for the sodium and zinc ionomers plotted as a function of shear rate and temperature. The curves are model predictions based on measurements in a capillary rheometer. While the zinc Surlyn has a higher viscosity than the sodium resin at 160°C, the viscosities are closely matched at higher temperatures typically experienced in the melt mixing zones of the extruder. The ZSK-18mm extruder has a high surface area to free volume providing significant heat transfer to control melt temperature. Masterbatches containing 25 wt. % MMT were prepared by melt compounding with the melt mixing zone barrels set to 160 and 220°C to impose high and low stress states on the sodium ionomer clay mixtures. The concentrate pellets were then co-fed with the sodium ionomer in a second extrusion operated with barrels set to a conventional profile to produce 3, 5 and 7 wt. % MMT nanocomposites.

Figure 2 shows tensile properties of the letdown compositions as a function of MMT loading and masterbatch process barrel temperature. Paul showed that the tensile modulus of MMT nanocomposites is influenced by the extent of exfoliation as indicated by a measurement or estimate of an effective aspect ratio [3-6]. The low temperature states show a clear increase in modulus over the high temperature states. From the rheology measurements, the shear stress at the 160°C condition would be significantly higher than at 210°C. It is likely that more tactoids would experience the critical stress required to overcome the cohesive force to exfoliate plate lets or split tactoid fragments. The elongation at break also changed with masterbatch compounding barrel temperature. The low temperature condition resulted in a decrease in the strain at break with MMT loading. For the high temperature state, the elongations were higher.

Another experiment was conducted to explore the effects of throughput (Q) and screw speed (N) on MMT dispersion in the sodium ionomer. Cloisite 20A was metered into the first feed port or the side stuffer at 3, 5, 7 and 10 wt. % MMT content. Two constant Q/N conditions were run. Tensile properties of injection molded samples are shown in Figure 3. Clay fed in the rear of the extruder experienced the high stress of the melting zone. This likely changed the extent of exfoliation and the effective aspect ratio as indicated by the tensile modulus. For each feed method, the modulus and elongations for almost all composition states were very similar at the constant Q/N conditions.

From Figure 1, the shear stress at a screw speed of 700 RPM is slightly higher than at 350 RPM. The energy dissipation, and hence the melt temperature are anticipated to be higher at 700 RPM, reducing the average stress in the channel. The mean residence time at 4.5 kg/hr (10 lb/hr) and 350 RPM is expected to be longer than at the 9.2 kg/hr (20 lb/hr) and 700 RPM condition [7, 8]. It is likely that the dispersion quality was similar for the two conditions with the same degree of fill. This result indicates that a melt compounding process can be operated in different regimes where a balance of residence time, stress and melt temperature can be found to produce the microstructures with similar physical properties.

Thermodynamic and Structural Effects

The choice of MMT surface modifier and the excess amount of surfactant above the clay cation exchange capacity (CEC) have significant effects on processing, dispersion and physical properties. Figure 4 shows the die hand melt temperature and exit pressure as a function modifier type and MMT concentration at the 4.5 kg/hr (10 lb/hr) and 350 RPM condition. Temperature and pressure increased with loading for Cloisite 20A [$M_2(HT)_2$ modifier, CEC 95 milli-equivalents/100gm clay (meq)]. The temperate and pressure increase with filler loading was reduced when excess surfactant was applied (Cloisite 15A, CEC 125 meq, and 6A, CEC 140 meq). This indicates that the excess modifier may act as a plasticizer. Excess surfactant likely dispersed in the polymer, reducing melt viscosity. Thermogravimetric analysis (TGA) tests on the organically modified MMT and sodium ionomer nanocomposites are shown in Figure 15. The TGA in air show that the clays and nanocomposites are thermally stable up to the process temperatures experienced in the extrusion tests (typically less than 240°C). The Cloisite 15A and 6A did show more weight loss, due to the free excess surfactant. Although is known that quaternary ammonium salts degrade through Hoffman elimination beginning at 160 to 170°C, the potential degradation products of the bound and excess surfactant did not appear to be a primary cause of plasticization (or additional discoloration of the samples). TEM micrographs in Figure 8 and 9 show that the Cloisite 20A and 15A composites with 5 wt. % MMT content had similar micro/nano-structures consisting of individual exfoliated platelets and a distribution of tactoids. For this experiment, the excess surfactant in the 15A clay did not improve the dispersion quality measurably. The tensile properties of the Cloisite 20A, 15A and 6A nanocomposites are shown in Figure 5. The modulus and elongations were very similar with MMT loading. The excess $M_2(HT)_2$ modifier may have improved the extent of

exfoliation (visually less haze) and hence, the effective aspect ratios slightly. Improved dispersion may have compensated for the plasticizing effect, especially with the Cloisite 6A (CEC 140 meq).

Cloisite 93A treated with a more polar modifier [MH(HT)2, CEC 90 meq] appeared to be thermodynamically incompatible with the sodium ionomer as indicated by decreasing process melt temperatures and pressures shown in Figure 4. Higher filler loading should have increased melt viscosity. If the exfoliation process produced a particle size distribution capable of forming a rheologically percolating network, the melt viscosity should have increased significantly [1]. The TGA data in Figure 15 show that the Cloisite 93A clay and the nanocomposite were thermally stable over the processing temperatures experienced. The sodium ionomer / 93A composite was more thermally stable than those using MMT modified with $M_2(HT)_2$. The TEM micrographs in Figure 10 show that the melt process failed to produce a good dispersion. The micro/nano-structure consisted of a small number of exfoliated platelets and a dominant population of large tactoids and agglomerates. This morphology resulted in little increase in the Young's modulus shown in Figure 5. However, Cloisite 93A composites had a significant increase in the elongation at break from 160 to 240%. Usually, a poor dispersion would not contribute to a large increase in the elongation (large agglomerate stress concentrators and flaw sites). This is strong indication that the $MH(HT)_2$ modifier was incompatible with the sodium Surlyn, resulting in poor interfacial adhesion which, in part, increased the toughness. Furthermore, the large tactoids could induce cavitation upon fracture, dissipating energy that could also increase the toughness [10]. This experiment shows that the thermodynamic compatibility between filler-modifier-polymer system components is critical in promoting good dispersion in the melt blending process and providing sufficient interfacial adhesion in the nanocomposites resulting in significant reinforcement [1].

In the next experiment, the zinc ionomer was melt compounded with the same set of MMT clays. Unmodified MMT (Cloisite Na+) was included in the composition series. All clays were introduced into the extruder in the side feed location. Figure 11 shows TEM micrographs of the zinc ionomer/Cloisite 20A (5 wt. % MMT) composite. While there is a small population of submicron particles, the dispersion represents a significant improvement in extent of exfoliation as compared with the sodium ionomer. The tensile properties are shown in Figure 6. The unmodified MMT control shows that without any surface modifier, the hydrophilic clay is incompatible with the ionomer resulting in a micron-scale dispersion (opaque bars with visible particles) and almost no reinforcement (very low effective aspect ratio). While the modulus increase trends are similar to the sodium ionomer system, the reinforcement was significantly higher for all compositions. Since the melt viscosity of the zinc and sodium ionomers have similar rheological properties, the data indicate that the divalent zinc Surlyn was more thermodynamic compatible with the $M_2(HT)_2$ modified clay, resulting in a superior morphology. This finding is consistent with the results reported by Paul [4- 6]. As with the sodium ionomer, while the excess $M_2(HT)_2$ modifier increased the inter-gallery spacing (to reduce the cohesive force), it did not make a measurable change to the tensile properties.

As shown in Figure 12, the more polar $MH(HT)_2$ modified Cloisite 93A produced a partially exfoliated micro/nano structure that was inferior to that of the Cloisite 20A sample. However, the dispersion quality of the zinc ionomer composite was far superior to that of the sodium ionomer system. The tensile data for both sodium and zinc ionomer nanocomposites are summarized in Figures 7. Zinc ionomer nanocomposites had significantly higher modulus over the entire composition space tested, but had lower toughness (energy to break) for most states. While it cannot yet be established why the zinc system produced a marked improvement over the sodium ionomer in dispersion and tensile properties, it is postulated that the zinc ionomer matrix was thermodynamically more compatible with both the $M_2(HT)_2$ and $MH(HT)_2$ surface modifiers. The effects of the ions on dispersion and surface interactions will be investigated in future research.

In the last experiment, several grades of $M_2(HT)_2$ modified Laponite synthetic Hectorite and Fluorohectorite layered silicates provided by Southern Clay Products were melt compounded into the zinc ionomer. Figure 13 shows TEM micrographs of a Laponite B Fluorohectorite composite with 5 wt. % clay content. Southern Clay Products claims that the platelet diameter is on the order of 25nm with a cation exchange capacity of 100 meq/100gm clay. WAXS measurements showed that the inter-gallery spacing was approximately 42Å, the largest of all silicates tested. This spacing was expected to reduce the platelet cohesive force substantially, increasing the likelihood of delamination in a polymer melt [1].

However, the dispersion was very poor, with much of the clay bound in large micron and sub-micron sized agglomerate particles. There were very few platelets found in the TEM micrographs and a sparse population of small tactoids was observed. Laponite RD Hectorite (25nm platelets, CEC of 75 meq) produced a very poor micronscale agglomerate dispersion as well. The bad dispersion made it difficult to produce useful TEM micrographs. Modified Laponite OG Hectorite (80 to 100nm platelets, CEC of 75meq) was compounded into the zinc ionomer with a resulting micro/nano-structure shown in the TEM micrographs of Figure 14. The TEM micrographs indicate that the dispersion was much better than that of both 25nm Laponite grades, but it was not as good as the 140 to 160nm platelet (presumed average sizes) Cloisite MMT composites.

The tensile properties of the Laponite composites are shown in Figure 6. The reinforcement with clay type and loading was consistent with the extent of exfoliation achieved during compounding and the silicate platelet size estimates. While the overall structure and surface charge mechanisms are similar for Hectorite, Fluorohectorite and MMT, slight surface charge distribution and chemistry differences may have affected dispersion kinematics and thermodynamic interactions. If one assumes that the van der Waals and ionic interactions were similar, then the test results indicate that platelet

dimensions influence melt compounding dispersion dynamics. These results would confirm Kamal's work showing how large lateral dimensions of platelets reduce the hydrodynamic stress required for breakup to occur in polymer melts [1, 9].

The structure-property relationships for the zinc ionomer nanocomposites were examined using composites theory [3-6]. The Halpin-Tsai equations were used to predict the Young's modulus and estimate an effective aspect ratio of the layered silicate dispersions as list in Table 1. Assuming good interfacial adhesion between the matrix and filler, the aspect ratios are consistent with the structures shown in the TEM micrographs and the tensile reinforcement. Unmodified MMT clay produced a micron-scale dispersion providing little reinforcement with an effective aspect ratio estimate, Af , of 5. The Cloisite 93A [$MH(HT)_2$] composites had an Af of 18, approximately half that of the $M_2(HT)_2$ modified MMT samples.

Conclusions

Melt compounding experiments were conducted on a twin screw extruder to disperse organically modified layered silicates into sodium and zinc ionomers. The results identified key factors that govern the exfoliation process in a polymer melt under shear that create the morphology and subsequently influence physical properties. These key factors include:
1) For the Surlyn ionomers tested, an appropriate organic modifier is required to provide thermodynamic compatibility in the melt state to promote a higher extent of exfoliation or tactoid size reduction while maximizing the effective aspect ratio of the particles.
2) Ethylene copolymers neutralized with different cations (sodium and zinc in these experiments) can alter the compatibility between the polymer and the modifier, resulting in significant changes to the morphology and tensile properties.
3) The stress generated during melt compounding does affect exfoliation and tactoid size reduction. On a laboratory extruder, barrel temperatures can be used effectively to change the melt viscosity and move the melt mixing zone from high to low stress states.
4) Layered silicate geometry (platelet size or aspect ratio) impacts the extent of exfoliation and tactoid size reduction. Layered silicates with large lateral platelet dimensions, like Montmorillonite, may be more easily dispersed in a polymer melt provided the components have good thermodynamic compatibility.

Further research is required to develop an understanding of the roles that the ionomer cations play in the thermodynamic interactions between the filler, modifier and polymer.

Acknowledgements

The author is grateful to Southern Clay Products (SCP) who produced the organically modified clays. The author acknowledges the advice and stimulating conversations with Doug Hunter at SCP and Professor Don Paul at the University of Texas at Austin.

References

1) S. N. Bhattacharya, R. K. Gupta, M. R. Kamal, "Polymeric Nanocomposites, Theory and Practice," Hanser Gardner, Cincinnati, 2008, 35-104.
2) D. L. Hunter, K. W. Kamena, D. R. Paul, MRS Bulletin, Volume 32, April 2007, 323-327.
3) T. D. Fornes, D. R. Paul, Polymer 44 (2003) 4993– 5013.
4) R. K. Shah, D. R. Paul, Polymer 46, 2005, 2646– 2662.
5) R. K. Shah, D. R. Paul, Macromolecules, 39, 2006, 3327-3336.
6) L. Cui, C. Troeltzsch, P. J. Yoon, D. R. Paul, Macromolecules, March, 2009.
7) J. Gao, G. Walsh, D. Bigio, R. Briber, M. Wetzel, AIChE Journal, 1999, 45, 2541-2549.
8) J. Gao, G. Walsh, D. Bigio, M. Wetzel, Polymer Engineering and Science, 40, 2000, 227-237.
9) N. Borse, M. Kamal, Polymer Engineering and Science, 49, 4, 2009, 641-650.
10) K. Wang, L. Chen, J. Wu, M. L. Toh, C. He, A. F. Yee, Macromolecules, 38, 2005, 788-800

Material	Est. Platelet Length (nm)	Est. Platelet Thickness (nm)	Modifier	Modifer Exchange (meq/100g clay)	% Moisture	% Weight Loss on Ignition	Modifier Anion	WAXS Gallery Spacing (nm)	Zn ionomer composite Halpin-Tsai Aspect Ratio (A_f)
Cloisite Na+	140	1.00	-	cec = 92	4-9%	7.0%	-	1.17	5.0
Cloisite 20A	140	1.00	$M_2(HT)_2$	95	<2%	38.0%	Chloride	2.41	33.0
Cloisite 15A	140	1.00	$M_2(HT)_2$	125	<2%	43.0%	Chloride	3.15	35.0
Cloisite 6A	140	1.00	$M_2(HT)_2$	140	<2%	48.0%	Chloride	3.51	35.0
Cloisite 93A	140	1.00	$MH(HT)_2$	90	<2%	37.5%	HSO_4	2.36	18.0
Laponite B Fluorohectorite	25	0.92	$M_2(HT)_2$	100	1.7%	41.2%	Chloride	4.23	6.0
Laponite RD Hectorite	25	0.92	$M_2(HT)_2$	75	1.2%	35.3%	Chloride	1.84	5.0
Laponite OG Hectorite	100	0.92	$M_2(HT)_2$	75		34.5%	Chloride	2.03	10.0

Table 1. Layered silicate properties (source Southern Clay Products and WAXS measurements).

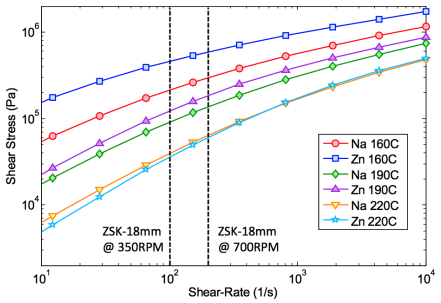

Figure 1. Sodium and zinc ionomer shear stress vs. shear rate curves at different operating temperature regimes.

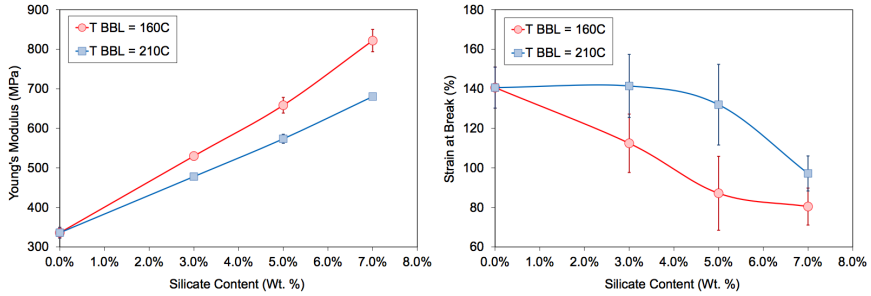

Figure 2. Tensile properties of injection molded bars of letdown extrusions of Sodium ionomer / Cloisite 20A master-batches made under low and high temperature conditions (error bars are ± one standard deviation, 6 bars per state).

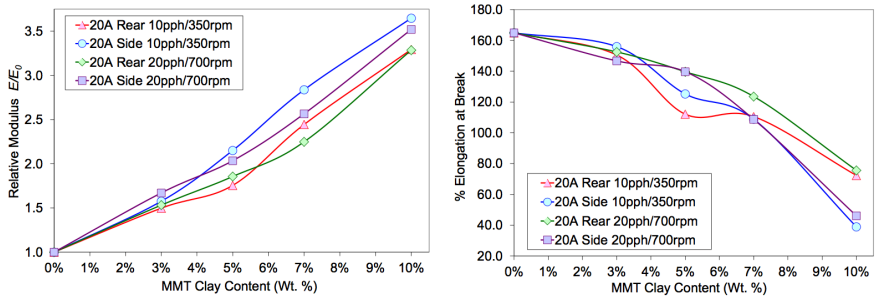

Figure 3. Tensile properties for constant Q/N samples run on a ZSK-18mm extruder with MMT fed in the rear or side ports.

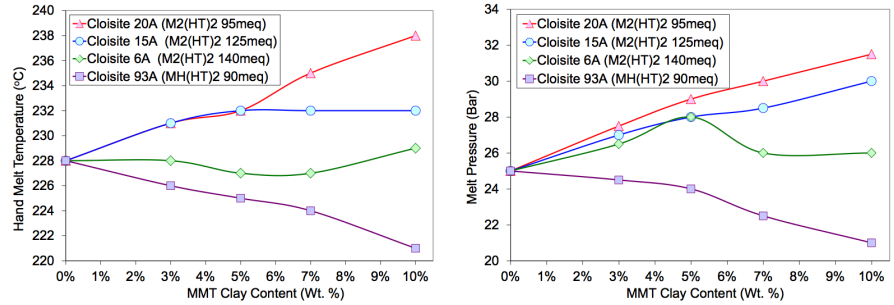

Figure 4. Sodium ionomer / organically modified MMT extrusion melt temperature and pressure.

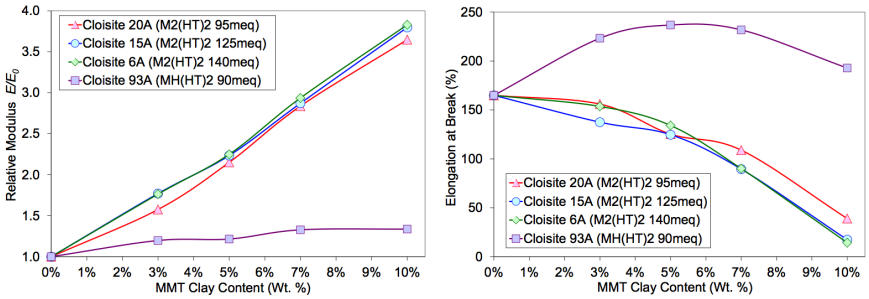

Figure 5. Sodium ionomer / organically modified MMT tensile properties.

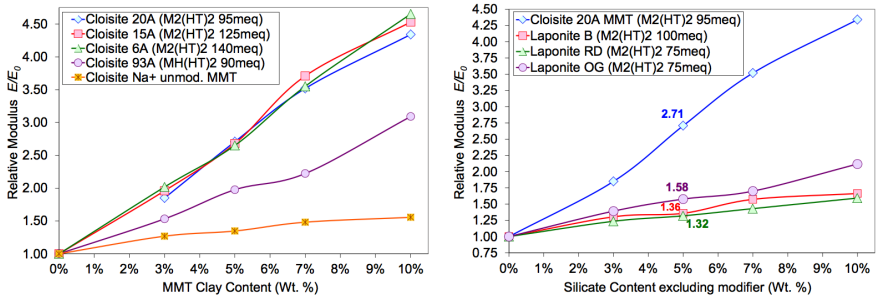

Figure 6. Tensile modulus data for zinc ionomer / layered silicate composites.

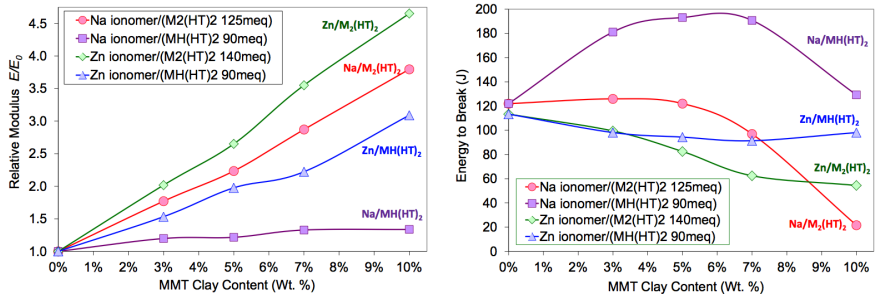

Figure 7. Tensile data comparing zinc and sodium ionomer / Cloisite MMT nanocomposites.

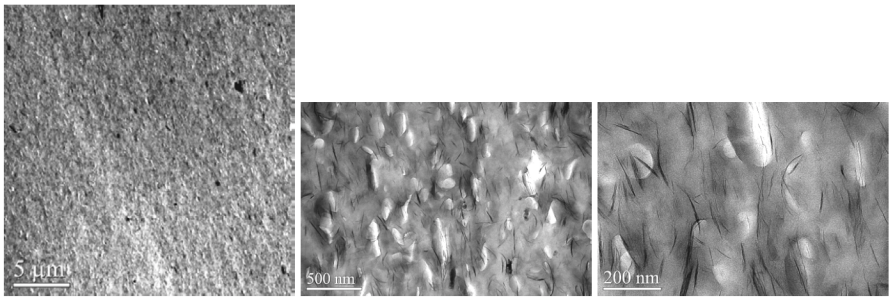

Figure 8. TEM images of sodium ionomer/Cloisite 20A (5 wt. % MMT) composite molded bar (10 lb/hr and 350RPM).

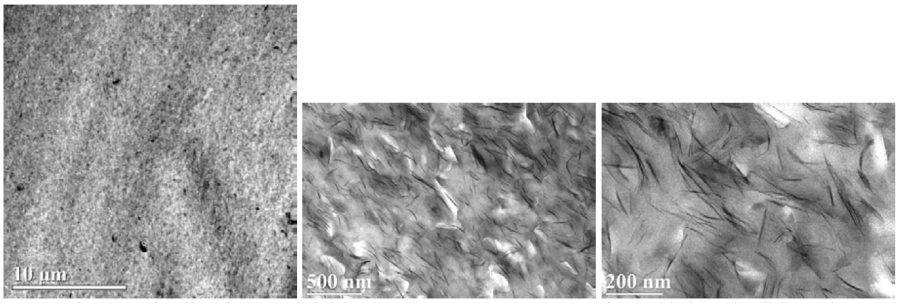

Figure 9. TEM images of sodium ionomer/Cloisite 15A (5 wt. % MMT) composite molded bar (10 lb/hr and 350RPM).

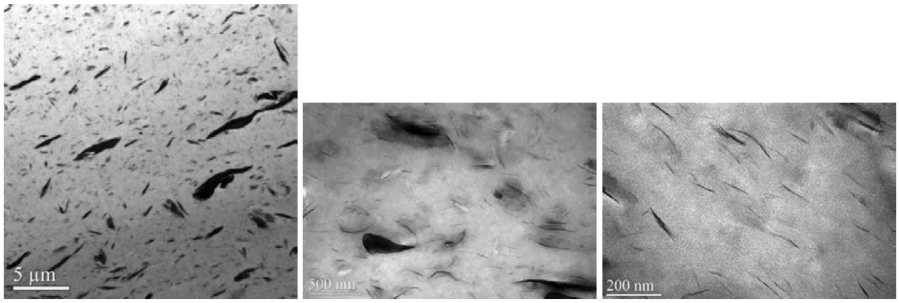

Figure 10. TEM images of sodium ionomer/Cloisite 93A (5 wt. % MMT) composite molded bar (10 lb/hr and 350RPM).

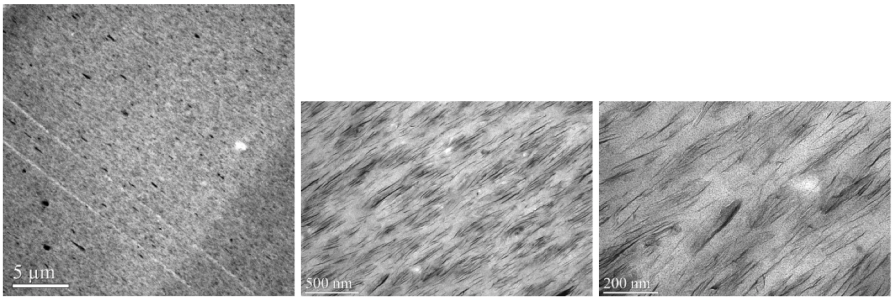

Figure 11. TEM images of zinc ionomer / Cloisite 20A (5 wt. % MMT).

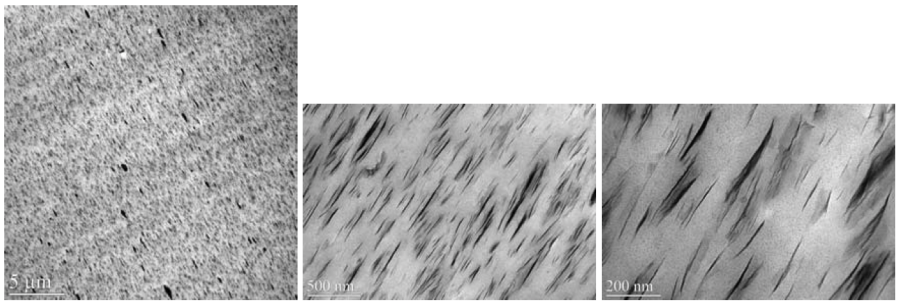

Figure 12. TEM images of zinc ionomer / Cloisite 93A (5 wt. % MMT).

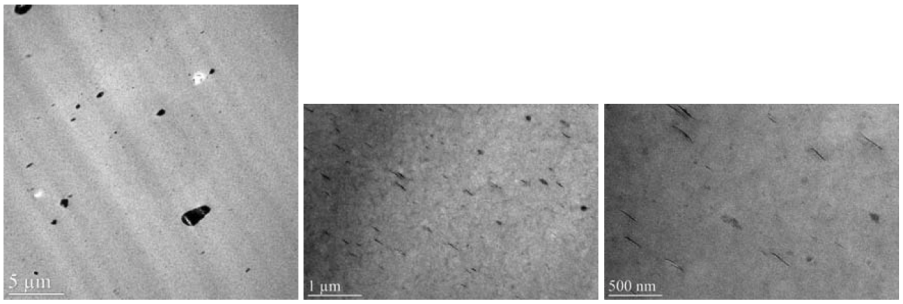

Figure 13. Zinc ionomer / organically modified Laponite B Fluorohectorite composite (5 wt. % clay) TEM.

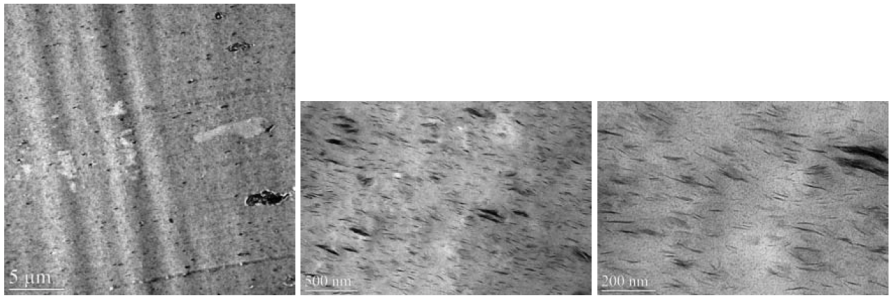

Figure 14. Zinc ionomer / organically modified Laponite OG composites (5 wt. % clay) TEM.

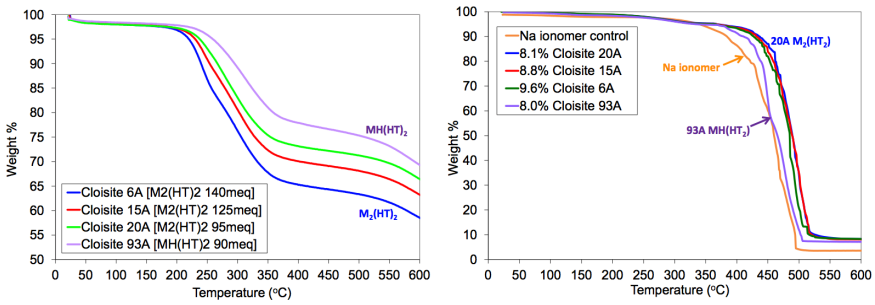

Figure 15. Thermogravimetric analysis (TGA) of organically modified MMT and sodium ionomer nanocomposites in air.